

Continuous variable entanglement swapping and its local certification: entangling distant mechanical modes

Mehdi Abdi,¹ Stefano Pirandola,² Paolo Tombesi,³ and David Vitali³

¹*Department of Physics, Iran University of Science and Technology, Tehran, Iran*

²*Department of Computer Science, University of York, York, United Kingdom*

³*School of Science and Technology, Physics Division, University of Camerino, Camerino, Italy*

(Dated: March 9, 2018)

We introduce a modification of the standard entanglement swapping protocol where the generation of entanglement between two distant modes is realized and verified using only local optical measurements. We show, indeed, that a simple condition on the purity of the initial state involving also an ancillary mode is sufficient to guarantee the success of the protocol by local measurements [M. Abdi *et al.*, *Phys. Rev. Lett.* **109**, 143601 (2012)]. We apply the proposed protocol to a tripartite optomechanical system where the never interacting mechanical modes become entangled and certified using only local optical measurements.

PACS numbers: 42.50.Ex, 03.67.Bg, 42.50.Wk, 03.65.Ta

I. INTRODUCTION

In quantum information networks, entanglement is a key feature for secure exchange of information [1–4]. There are many proposals and realizations for generating entanglement between various nodes of a quantum network; entanglement of two trapped ions [5], two atoms [6, 7], two macroscopic diamonds at room temperature [8] just to quote a few of them, up to the most recent distribution of entanglement between distant sites, as across a lake [9] or between two islands [10]. However, most proposals require preparation through a physical, direct [11] or indirect [12], interaction. Entanglement swapping, instead, is one of the most surprising effects of the non-locality of quantum mechanics because it is a way to create entanglement, i.e., quantum correlations, between distant parties that never interacted [13]. For continuous variables, which we are here interested in, this technique was experimentally demonstrated in Refs. [14, 15].

For nontrivial quantum communication tasks such as teleportation [2, 16], it is necessary to ensure that the remote sites which are the ends of the quantum channel are entangled. This condition may lead to serious difficulties, since it requires test measurements on the remote sites, which could be difficult to perform. Therefore, it is important to test the success of a swapping protocol in easier ways. In this paper we provide a solution to such a requirement, i.e., we propose a protocol which makes it possible to test the entanglement between remote nodes employing local optical measurements only. Although our protocol imposes a condition on the initially prepared states, from a practical point of view this is a reasonable cost to pay for. Such a protocol can be utilized for producing confident quantum channels between two far and non-interacting nodes, e.g., two satellites, by measurements in halfway for both creating and testing it (cf. Fig. 1(b)). Moreover, this protocol provides a promising method for experimentally creating entanglement between two macroscopic objects in direction of

questioning the so called Schrodinger cat states and their decoherence [17–19]. From this point of view, this work extends Ref. [20], which first pioneered the possibility to use entanglement swapping for entangling two massive systems, such as two micromechanical oscillators.

In this paper the matrices are shown by curly capital letters, while the vectors are in bold face letters. The paper is organized as follows: In Sec. II we explain the protocol. In Sec. III we discuss the output state resulting from running the protocol. Then, the protocol is applied in the specific case of optomechanical systems in Sec. IV. Concluding remarks are provided in Sec. V.

II. THE PROTOCOL

The initial states employed in this protocol, on both sides of the system, are tripartite continuous variable states. In fact, the standard entanglement swapping protocol is modified by adding an ancillary mode to each side in order to provide the local certification of the achieved entanglement between the two remote sites. In Fig. 1(a) the principles of the protocol is sketched.

A. Initial state

The whole system is initially composed of a pair of independent tripartite entangled bosonic modes, one possessed by Alice and one by Bob. Alice and Bob are located at remote sites, prepare a *specific* tripartite state, and each shares two modes with Charlie, who is located for simplicity halfway between them (see Fig. 1(a) and (b)). These four bosonic modes (two modes from each side) will be manipulated by Charlie when executing the protocol. Since the two initial subsystems of Alice and Bob are independent and non-interacting, the initial state of the whole system can be described by the tensor product of the two initial tripartite states, $\rho_1 \otimes \rho_2$ where

ρ_1 and ρ_2 are shared by Alice–Charlie and Bob–Charlie, respectively. We identify the modes remained at each side (the ‘remote’ modes) by the bosonic annihilation operators \hat{a}_l with commutation relation $[\hat{a}_l, \hat{a}_{l'}^\dagger] = \delta_{ll'}$. The bosonic modes used for the Bell measurement and certifying process are described by \hat{b}_l , and \hat{c}_l with similar commutators, respectively, where $l = 1$ stands for Alice, while $l = 2$ is related to Bob. In the case of an optomechanical system which we will consider later on, the remote mode will be represented by a mechanical mode of a micro-mirror and the modes shared with Charlie by two output modes of the optical cavity (see Fig. 1(c)).

The tripartite initial state at each site must be prepared in a proper way, in order to achieve the desired state at the end of the swapping protocol. That is, the final resulting state should give an entangled state between the remote modes and provide a trustful way to endorse it by the two ancillary, certifying, modes. This is satisfied when, in the output state, the remote modes are more entangled than the certifying modes, $E_N^R > E_N^C$, where E_N is an entanglement monotone that in this paper is chosen to be the logarithmic negativity [21]. In the following we shall derive an explicit condition for these certifying tripartite states [22].

In the Wigner function formalism, the initial state is expressed by the product of the Wigner function of the states at each site,

$$W_{\text{in}}(\alpha_1, \alpha_2, \beta_1, \beta_2, \gamma_1, \gamma_2) = W_1(\alpha_1, \beta_1, \gamma_1)W_2(\alpha_2, \beta_2, \gamma_2), \quad (1)$$

where we have introduced the complex phase space variable $\alpha_l \equiv (x_{al} + ip_{al})/\sqrt{2}$ corresponding to the bosonic mode operator \hat{a}_l and the same is done for the other modes, $\hat{b}_l \leftrightarrow \beta_l$ and $\hat{c}_l \leftrightarrow \gamma_l$ with $l = 1, 2$. The real phase space variables x_{kl} and p_{kl} with $k = a, b, c$ and $l = 1, 2$ are the counterparts of the Hermitian quadrature operators \hat{x}_{lk} and \hat{p}_{lk} satisfying the commutation relations

$$[\hat{x}_{kl}, \hat{p}_{k'l'}] = i\delta_{kk'}\delta_{ll'}.$$

B. Bell measurement

In order to convert Alice–Charlie and Bob–Charlie entanglement to the nonlocal Alice–Bob entanglement, Charlie must erase some of the information shared with Alice and Bob. This is obtained via the CV version of the Bell measurement, which we recall here.

Beam-splitter mixing— Charlie mixes one mode from each side (here labeled as \hat{b}_1 and \hat{b}_2) through a balanced beam-splitter, performing the following linear transformation for the annihilation operators

$$\begin{bmatrix} \hat{b}_+ \\ \hat{b}_- \end{bmatrix} = \frac{1}{\sqrt{2}} \begin{bmatrix} 1 & 1 \\ -1 & 1 \end{bmatrix} \begin{bmatrix} \hat{b}_1 \\ \hat{b}_2 \end{bmatrix}, \quad (2)$$

where \hat{b}_\pm refer to the output modes \pm of the beam-splitter. At the level of quadratures one has

$$\hat{x}_\pm = \frac{\hat{x}_{b2} \pm \hat{x}_{b1}}{\sqrt{2}}, \quad \hat{p}_\pm = \frac{\hat{p}_{b2} \pm \hat{p}_{b1}}{\sqrt{2}}, \quad (3)$$

while the phase space counterpart of this bilinear transformation is

$$\beta_\pm = \frac{\beta_2 \pm \beta_1}{\sqrt{2}},$$

where $\beta_\pm \equiv (x_\pm + ip_\pm)/\sqrt{2}$ are the complex phase-space variables associated with the beam-splitter output variables.

Homodyne detection.— Charlie measures the \hat{x}_- and \hat{p}_+ quadratures with two homodyne detectors, getting the outcomes $\{\tilde{x}_-, \tilde{p}_+\} = \sqrt{2}\{\tilde{\beta}_-^{\Re}, \tilde{\beta}_+^{\Im}\}$ with probability $P(\tilde{x}_-, \tilde{p}_+)$, where the superscripts \Re and \Im correspond to the real and imaginary part of the complex number or variable. This measurement leads to the conditional collapse of the initial six-mode state into a four-mode state:

$$W_{\text{in}} \longrightarrow P(\tilde{x}_-, \tilde{p}_+)^{-1} W_{\text{in}} \delta(\beta_-^{\Re} - \tilde{\beta}_-^{\Re}) \delta(\beta_+^{\Im} - \tilde{\beta}_+^{\Im}). \quad (4)$$

The conditional output state generated at this stage is obtained by tracing out the beam-splitter output modes \pm , i.e., by integrating the collapsed state Wigner function over the variables β_+ and β_- , which reads

$$W_{\text{con}}(\alpha_1, \alpha_2, \gamma_1, \gamma_2 | \tilde{\beta}_-^{\Re}, \tilde{\beta}_+^{\Im}) = \frac{1}{P(\tilde{\beta}_-^{\Re}, \tilde{\beta}_+^{\Im})} \times \int d\beta_-^{\Im} \int d\beta_+^{\Re} W_{\text{in}}(\alpha_1, \alpha_2, \gamma_1, \gamma_2, \beta_+, \beta_-) |_{\beta_-^{\Re}=\tilde{\beta}_-^{\Re}, \beta_+^{\Im}=\tilde{\beta}_+^{\Im}}. \quad (5)$$

By introducing $\tilde{\beta} \equiv i\tilde{p}_+ - \tilde{x}_- = \sqrt{2}(i\tilde{\beta}_+^{\Im} - \tilde{\beta}_-^{\Re})$, which is a complex number representing the measurement outcomes in a compact form, and $\beta \equiv [x_+ + i\tilde{p}_+ - (\tilde{x}_- + ip_-)]/2$ which is actually equal to $\beta_1 |_{\{\tilde{x}_-, \tilde{p}_+\}}$ (i.e., β_1 specified

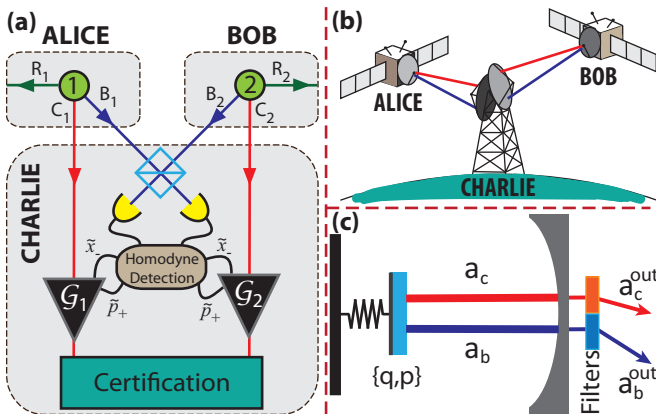


FIG. 1. (Color online) (a) Scheme of the entanglement swapping protocol with local certification. (b) Schematic quantum communication scenario in which the generalized entanglement swapping protocol applies. (c) The optomechanical setup which can be mounted on each remote site.

by the measurement outcomes) we arrive at the following compact form for the conditional state after the Bell measurement

$$W_{\text{con}}(\alpha_1, \alpha_2, \gamma_1, \gamma_2 | \tilde{\beta}) = \frac{1}{P(\tilde{\beta})} \int d^2 \beta W_1(\alpha_1, \gamma_1, \beta) \times W_2(\alpha_2, \gamma_2, \beta^* - \tilde{\beta}^*). \quad (6)$$

Eq. (6) has been obtained using the fact that $\beta_2 | \{\tilde{x}_-, \tilde{p}_+\} = \beta^* - \tilde{\beta}^*$, the property

$$P(\tilde{\beta}_{-}^{\Re}, \tilde{\beta}_{+}^{\Im}) = P(\tilde{\beta}_{-}^{\Re} | \tilde{\beta}_{+}^{\Im}) P(\tilde{\beta}_{+}^{\Im}), \quad (7)$$

and that $\tilde{\beta}^{\Re} = -\sqrt{2}\tilde{\beta}_{-}^{\Re}$ and $\tilde{\beta}^{\Im} = \sqrt{2}\tilde{\beta}_{+}^{\Im}$. Moreover, we have also exploited the fact that $P(ky) = P(y)/|k|$ for $k \in \mathbb{R}$, so that

$$P(\tilde{\beta}_{-}^{\Re}, \tilde{\beta}_{+}^{\Im}) = \sqrt{2}P(\tilde{\beta}_{-}^{\Re} | \tilde{\beta}_{+}^{\Im}) \sqrt{2}P(\tilde{\beta}_{+}^{\Im}) = 2P(\tilde{\beta}^{\Re}, \tilde{\beta}^{\Im}) \equiv 2P(\tilde{\beta}), \quad (8)$$

and that $\int d\beta_{-}^{\Im} \int d\beta_{+}^{\Re} \leftrightarrow 2 \int d^2 \beta$.

C. Classical communication

The conditional state of Eq. (6) has a fluctuating displacement associated with the outcome of the Bell measurement. Charlie broadcasts the measurement results, so that Charlie himself, as well as Alice and Bob, may suitably displace their modes according to the measurement outcomes. In the Heisenberg picture, these displacements, which will complete the swapping process, are [23]

$$\begin{cases} \hat{x}_{a1} \rightarrow \hat{x}_{a1} + \sqrt{2} \tilde{x}_{-} \\ \hat{p}_{a1} \rightarrow \hat{p}_{a1} + \sqrt{2} \tilde{p}_{+} \end{cases}, \quad (9a)$$

$$\begin{cases} \hat{x}_{a2} \rightarrow \hat{x}_{a2} - \sqrt{2} \tilde{x}_{-} \\ \hat{p}_{a2} \rightarrow \hat{p}_{a2} + \sqrt{2} \tilde{p}_{+} \end{cases}, \quad (9b)$$

$$\begin{cases} \hat{x}_{c1} \rightarrow \hat{x}_{c1} + \sqrt{2} \tilde{x}_{-} \\ \hat{p}_{c1} \rightarrow \hat{p}_{c1} + \sqrt{2} \tilde{p}_{+} \end{cases}, \quad (9c)$$

$$\begin{cases} \hat{x}_{c2} \rightarrow \hat{x}_{c2} - \sqrt{2} \tilde{x}_{-} \\ \hat{p}_{c2} \rightarrow \hat{p}_{c2} + \sqrt{2} \tilde{p}_{+} \end{cases}. \quad (9d)$$

However, in practice, Alice, Bob, and Charlie may employ gain factors in displacing their modes [24]. As it will be discussed in Sec. III, application of these gain factors may be useful for improving the quality of the swapped entanglement. In terms of the complex phase space variables, these conditional displacements can be expressed

as

$$\alpha_1 \rightarrow \alpha_1 + \tilde{\beta}_{a1}^*, \quad (10a)$$

$$\alpha_2 \rightarrow \alpha_2 - \tilde{\beta}_{a2}, \quad (10b)$$

$$\gamma_1 \rightarrow \gamma_1 + \tilde{\beta}_{c1}^*, \quad (10c)$$

$$\gamma_2 \rightarrow \gamma_2 - \tilde{\beta}_{c2}, \quad (10d)$$

where the displacement of each mode when phase-sensitive gain factors are used are given by

$$\tilde{\beta}_{a1} = -g_{a1}^{\Re} \tilde{x}_{-} + i g_{a1}^{\Im} \tilde{p}_{+}, \quad (11a)$$

$$\tilde{\beta}_{a2} = -g_{a2}^{\Re} \tilde{x}_{-} + i g_{a2}^{\Im} \tilde{p}_{+}, \quad (11b)$$

$$\tilde{\beta}_{c1} = -g_{c1}^{\Re} \tilde{x}_{-} + i g_{c1}^{\Im} \tilde{p}_{+}, \quad (11c)$$

$$\tilde{\beta}_{c2} = -g_{c2}^{\Re} \tilde{x}_{-} + i g_{c2}^{\Im} \tilde{p}_{+}. \quad (11d)$$

In practice, the process is run continuously with measurement outcomes changing in time, so that the conditional state W_{con} of Eq. (6) is transformed into a displaced state W_{dis} according to Eqs. (10) with probability $P(\tilde{\beta})$. In general, the state of the system is therefore given by the ensemble average

$$W_{\text{ens}}(\alpha_1, \alpha_2, \gamma_1, \gamma_2) = \int d^2 \tilde{\beta} P(\tilde{\beta}) W_{\text{dis}}(\alpha_1, \alpha_2, \gamma_1, \gamma_2 | \tilde{\beta}). \quad (12)$$

We remark that this average is superfluous if the displacements are optimal, such to transform W_{con} into a zero-mean state [20]. As we will see afterwards, this reduction is also exploited in our approach.

III. THE OUTPUT STATE

The output state of the swapping protocol is described by Eq. (12) which completely characterizes the final state of the system and is given by a convolution integral of the Wigner functions of the factorized initial state, evaluated at appropriate phase space points. For this reason it is convenient to express the output state in terms of its symmetrically-ordered characteristic function which is just the Fourier transform of the Wigner function, $\Phi(\lambda_1, \lambda_2, \mu_1, \mu_2) = \text{FT}[W(\alpha_1, \alpha_2, \gamma_1, \gamma_2)]$, obtaining

$$\Phi_{\text{ens}}(\lambda_1, \lambda_2, \mu_1, \mu_2) = \Phi_1(\lambda_1, \mu_1, \nu) \Phi_2(\lambda_2, \mu_2, \nu^*), \quad (13)$$

where λ_k and μ_k are the conjugate variables for α_k and γ_k in the Wigner function, while the correlations between the four modes are contained in the complex variable ν given by

$$\nu \equiv g_{a1}^{\Im} \lambda_1^{\Re} + g_{c1}^{\Im} \mu_1^{\Re} + g_{a2}^{\Im} \lambda_2^{\Re} + g_{c2}^{\Im} \mu_2^{\Re} + i(g_{a2}^{\Re} \lambda_2^{\Im} + g_{c2}^{\Re} \mu_2^{\Im} - g_{a1}^{\Re} \lambda_1^{\Im} - g_{c1}^{\Re} \mu_1^{\Im}). \quad (14)$$

In order to perform calculations, it is convenient to adopt a vector notation in which we associate to each complex variable a two-dimensional real vector according to

$$\lambda = \lambda^{\Re} + i \lambda^{\Im} \longleftrightarrow \boldsymbol{\lambda} \equiv [\lambda^{\Im}, -\lambda^{\Re}]^{\text{T}}. \quad (15)$$

As a consequence, the characteristic functions in Eq. (13) can be rewritten as

$$\Phi_1(\lambda_1, \mu_1, \nu) \longleftrightarrow \Phi_1(\lambda_1, \mu_1, \mathcal{G}_{a1}\lambda_1 + \mathcal{G}_{a2}\lambda_2 + \mathcal{G}_{c1}\mu_1 + \mathcal{G}_{c2}\mu_2), \quad (16)$$

$$\Phi_2(\lambda_2, \mu_2, \nu^*) \longleftrightarrow \Phi_2(\lambda_2, \mu_2, -\mathcal{Z}\mathcal{G}_{a1}\lambda_1 - \mathcal{Z}\mathcal{G}_{a2}\lambda_2 - \mathcal{Z}\mathcal{G}_{c1}\mu_1 - \mathcal{Z}\mathcal{G}_{c2}\mu_2), \quad (17)$$

where $\mathcal{Z} \equiv \text{diag}[1, -1]$ and we have introduced the following gain matrices

$$\mathcal{G}_{a1} \equiv \begin{bmatrix} -g_{a1} & 0 \\ 0 & h_{a1} \end{bmatrix}, \quad \mathcal{G}_{a2} \equiv \begin{bmatrix} g_{a2} & 0 \\ 0 & h_{a2} \end{bmatrix}, \quad (18)$$

$$\mathcal{G}_{c1} \equiv \begin{bmatrix} -g_{c1} & 0 \\ 0 & h_{c1} \end{bmatrix}, \quad \mathcal{G}_{c2} \equiv \begin{bmatrix} g_{c2} & 0 \\ 0 & h_{c2} \end{bmatrix}. \quad (19)$$

A. The case of initial tripartite Gaussian states

We now restrict to the physically relevant case when the two independent tripartite states ρ_1 and ρ_2 at Alice and Bob sites are Gaussian. For the class of Gaussian states, the characteristic function is completely determined by the first and second moments of the quadrature operators [2]. In fact, for an N -mode Gaussian state, the characteristic function is equal to $\Phi(\mathbf{k}) = \exp\{-\mathbf{k}^T \mathcal{V} \mathbf{k} / 2 + i \mathbf{d}^T \mathbf{k}\}$, where \mathcal{V} and \mathbf{d} are the covariance matrix (CM) and displacement vector of the state, respectively, and $\mathbf{k} = [x_1, p_1, \dots, x_N, p_N]^T$ is the vector of

phase space variables. The entanglement properties of the final state are fully determined by the CM because the displacement affects only local properties.

We consider two initial tripartite Gaussian states with zero displacement and characterized by the following CM

$$\mathcal{V}_k = \begin{bmatrix} \mathcal{R}_k & \mathcal{D}_k & \mathcal{F}_k \\ \mathcal{D}_k^T & \mathcal{B}_k & \mathcal{E}_k \\ \mathcal{F}_k^T & \mathcal{E}_k^T & \mathcal{C}_k \end{bmatrix}, \quad k = 1, 2, \quad (20)$$

which is expressed in terms of its 2×2 sub-blocks. By inserting the corresponding characteristic functions into Eq. (13), one gets for the ensemble-averaged output state a four-mode Gaussian state with vanishing first moments and a CM given by

$$\mathcal{V}_{\text{in}} = \begin{bmatrix} \mathcal{V}_1 & \\ & \mathcal{V}_2 \end{bmatrix} \longrightarrow \mathcal{V}_{\text{ens}} = \begin{bmatrix} \mathcal{V}'_{\text{R}} & \mathcal{V}'_{\text{X}} \\ \mathcal{V}'_{\text{X}}^T & \mathcal{V}'_{\text{C}} \end{bmatrix}. \quad (21)$$

In particular, the CM of the interesting bipartite subsystems (Alice–Bob and the certifying modes) are given by

$$\mathcal{V}'_{\text{R}} = \begin{bmatrix} \mathcal{R}_1 & \\ & \mathcal{R}_2 \end{bmatrix} + \begin{bmatrix} \mathcal{G}_{a1}^T \mathcal{M} \mathcal{G}_{a1} + \mathcal{D}_1^T \mathcal{G}_{a1} + \mathcal{G}_{a1}^T \mathcal{D}_1 & \mathcal{G}_{a1}^T \mathcal{M} \mathcal{G}_{a2} + \mathcal{D}_1^T \mathcal{G}_{a2} - \mathcal{G}_{a1}^T \mathcal{Z} \mathcal{D}_2 \\ \mathcal{G}_{a2}^T \mathcal{M} \mathcal{G}_{a1} + \mathcal{G}_{a2}^T \mathcal{D}_1 - \mathcal{D}_2^T \mathcal{Z} \mathcal{G}_{a1} & \mathcal{G}_{a2}^T \mathcal{M} \mathcal{G}_{a2} - \mathcal{D}_2^T \mathcal{Z} \mathcal{G}_{a2} + \mathcal{G}_{a2}^T \mathcal{Z} \mathcal{D}_2 \end{bmatrix}, \quad (22)$$

$$\mathcal{V}'_{\text{C}} = \begin{bmatrix} \mathcal{C}_1 & \\ & \mathcal{C}_2 \end{bmatrix} + \begin{bmatrix} \mathcal{G}_{c1}^T \mathcal{M} \mathcal{G}_{c1} + \mathcal{E}_1^T \mathcal{G}_{c1} + \mathcal{G}_{c1}^T \mathcal{E}_1 & \mathcal{G}_{c1}^T \mathcal{M} \mathcal{G}_{c2} + \mathcal{E}_1^T \mathcal{G}_{c2} - \mathcal{G}_{c1}^T \mathcal{Z} \mathcal{E}_2 \\ \mathcal{G}_{c2}^T \mathcal{M} \mathcal{G}_{c1} + \mathcal{G}_{c2}^T \mathcal{E}_1 - \mathcal{E}_2^T \mathcal{Z} \mathcal{G}_{c1} & \mathcal{G}_{c2}^T \mathcal{M} \mathcal{G}_{c2} - \mathcal{E}_2^T \mathcal{Z} \mathcal{G}_{c2} + \mathcal{G}_{c2}^T \mathcal{Z} \mathcal{E}_2 \end{bmatrix}, \quad (23)$$

where we have introduced the matrix $\mathcal{M} \equiv \mathcal{B}_1 + \mathcal{Z} \mathcal{B}_2 \mathcal{Z}$.

B. Optimization of the output state

The ensemble average output state is of much less quality and less entangled than the initial state because of the average over the differently displaced states conditioned to the homodyne measurement outcome. However one can optimize the output state by optimizing the choice of the gain factors. It is quite evident that such an optimization corresponds to adjust the gain so that the displacement of the conditional state is always put to zero. In such a case the output state is no more blurred by the fluctuating measurement outcomes and the CM of the output state corresponds to that of the conditional state [20].

The first moment of the displaced conditional state can be obtained by calculating the characteristic function of

the Wigner function which is obtained from Eq. (6)

$$W_{\text{dis}} = \frac{1}{P(\tilde{\beta})} \int d^2 \beta W_1(\alpha_1 + \tilde{\beta}_{a1}^*, \gamma_1 + \tilde{\beta}_{c1}^*, \beta) \times W_2(\alpha_2 - \tilde{\beta}_{a2}, \gamma_2 - \tilde{\beta}_{c2}, \beta^* - \tilde{\beta}^*), \quad (24)$$

which is given by

$$\Phi_{\text{dis}}(\lambda_1, \lambda_2, \mu_1, \mu_2) = \frac{1}{\pi^2 P(\tilde{\beta})} \int d^2 \eta \Phi_1(\lambda_1, \mu_1, \eta^*) \times \exp\{-\mu_1 \tilde{\beta}_{c1} - \mu_1^* \tilde{\beta}_{c1}^*\} \Phi_2(\lambda_2, \mu_2, \eta) \times \exp\{\mu_2 \tilde{\beta}_{c2}^* - \mu_2^* \tilde{\beta}_{c2}\}. \quad (25)$$

Now let us switch to the vector notation, by defining the vector corresponding to the measurement outcome $\tilde{\beta} = [i\tilde{\beta}^{\text{R}}, -i\tilde{\beta}^{\text{I}}]$, so that this characteristic function can

be rewritten as

$$\Phi_{\text{dis}}(\boldsymbol{\lambda}_1, \boldsymbol{\lambda}_2, \boldsymbol{\mu}_1, \boldsymbol{\mu}_2) = \frac{\exp\left\{2\tilde{\boldsymbol{\beta}}^\top (\mathcal{Z}\mathcal{G}_{c1}\boldsymbol{\mu}_1 + \mathcal{Z}\mathcal{G}_{c2}\boldsymbol{\mu}_2)\right\}}{\pi^2 P(\tilde{\boldsymbol{\beta}})} \times \int d^2\boldsymbol{\eta} \exp\{2\tilde{\boldsymbol{\beta}}^\top \boldsymbol{\eta}\} \Phi_1(\boldsymbol{\lambda}_1, \boldsymbol{\mu}_1, -\mathcal{Z}\boldsymbol{\eta}) \Phi_2(\boldsymbol{\lambda}_2, \boldsymbol{\mu}_2, \boldsymbol{\eta}). \quad (26)$$

Since we have considered the initial state of each side to be a zero-displaced Gaussian state, whose CM is given by Eq. (20), we arrive at the following first moment vector for the displaced conditional state

$$\mathbf{d}_{\text{dis}} = -2i \begin{bmatrix} (\mathcal{G}_{a1}\mathcal{Z} + \mathcal{D}_1\mathcal{Z}\mathcal{M}^{-1})\tilde{\boldsymbol{\beta}} \\ (\mathcal{G}_{c1}\mathcal{Z} + \mathcal{E}_1\mathcal{Z}\mathcal{M}^{-1})\tilde{\boldsymbol{\beta}} \\ (\mathcal{G}_{c2}\mathcal{Z} - \mathcal{E}_2\mathcal{M}^{-1})\tilde{\boldsymbol{\beta}} \\ (\mathcal{G}_{a2}\mathcal{Z} - \mathcal{D}_2\mathcal{M}^{-1})\tilde{\boldsymbol{\beta}} \end{bmatrix}. \quad (27)$$

By applying the condition for the optimal output state, i.e. $\mathbf{d}_{\text{dis}} = \mathbf{0}$, from Eq. (27) we get

$$\mathcal{G}_{a1} = -\mathcal{Z}\mathcal{M}^{-1}\mathcal{Z}\mathcal{D}_1, \quad (28a)$$

$$\mathcal{G}_{a2} = \mathcal{Z}\mathcal{M}^{-1}\mathcal{D}_2, \quad (28b)$$

$$\mathcal{G}_{c1} = -\mathcal{Z}\mathcal{M}^{-1}\mathcal{Z}\mathcal{E}_1, \quad (28c)$$

$$\mathcal{G}_{c2} = \mathcal{Z}\mathcal{M}^{-1}\mathcal{E}_2, \quad (28d)$$

as the optimal values for the gain matrices. Finally, the CM of the optimally displaced (output) state reads

$$\mathcal{V}_{\text{out}} = \begin{bmatrix} \mathcal{V}_{\text{R}} & \mathcal{V}_{\text{X}} \\ \mathcal{V}_{\text{X}}^\top & \mathcal{V}_{\text{C}} \end{bmatrix}, \quad (29)$$

which is identical to the CM of the conditional state, expressed by the Wigner function in Eq. (6). Explicitly, the various blocks \mathcal{V}_{R} , \mathcal{V}_{C} , and \mathcal{V}_{X} are equal to [22]

$$\mathcal{V}_{\text{R}} = \begin{bmatrix} \mathcal{R}_1 - \mathcal{D}_1^\top \mathcal{Z}\mathcal{M}^{-1}\mathcal{Z}\mathcal{D}_1 & \mathcal{D}_1^\top \mathcal{Z}\mathcal{M}^{-1}\mathcal{D}_2 \\ \mathcal{D}_2^\top \mathcal{M}^{-1}\mathcal{Z}\mathcal{D}_1 & \mathcal{R}_2 - \mathcal{D}_2^\top \mathcal{M}^{-1}\mathcal{D}_2 \end{bmatrix}, \quad (30)$$

$$\mathcal{V}_{\text{C}} = \begin{bmatrix} \mathcal{C}_1 - \mathcal{E}_1^\top \mathcal{Z}\mathcal{M}^{-1}\mathcal{Z}\mathcal{E}_1 & \mathcal{E}_1^\top \mathcal{Z}\mathcal{M}^{-1}\mathcal{E}_2 \\ \mathcal{E}_2^\top \mathcal{M}^{-1}\mathcal{Z}\mathcal{E}_1 & \mathcal{C}_2 - \mathcal{E}_2^\top \mathcal{M}^{-1}\mathcal{E}_2 \end{bmatrix}, \quad (31)$$

$$\mathcal{V}_{\text{X}} = \begin{bmatrix} \mathcal{F}_1 - \mathcal{D}_1^\top \mathcal{Z}\mathcal{M}^{-1}\mathcal{Z}\mathcal{E}_1 & \mathcal{D}_1^\top \mathcal{Z}\mathcal{M}^{-1}\mathcal{E}_2 \\ \mathcal{D}_2^\top \mathcal{M}^{-1}\mathcal{Z}\mathcal{E}_1 & \mathcal{F}_2 - \mathcal{D}_2^\top \mathcal{M}^{-1}\mathcal{E}_2 \end{bmatrix}. \quad (32)$$

C. Standard form

To get an intuitive picture for determining the conditions under which the entanglement swapping with local certification protocol properly works we use the standard form of the CM. In fact, the CM of an arbitrary N -mode state expresses the covariances between the quadratures of the state, and, for this reason, it must respect the uncertainty principle. Therefore, we adopt the compact form of commutation relation for the vector of operators, $\hat{\mathbf{k}} = [\hat{x}_1, \hat{p}_1, \dots, \hat{x}_N, \hat{p}_N]^\top$, as $[\hat{\mathbf{k}}_l, \hat{\mathbf{k}}_m] = i\mathcal{J}_{lm}^{(N)}$, where

$$\mathcal{J}^{(N)} = \bigoplus_{k=1}^N \mathcal{J}_k, \quad \text{with } \mathcal{J}_k \equiv \begin{bmatrix} 0 & 1 \\ -1 & 0 \end{bmatrix}, \quad (33)$$

is the N -mode symplectic form. Thus, every CM must satisfy the following condition

$$\mathcal{V} + \frac{i}{2}\mathcal{J}^{(N)} \geq 0. \quad (34)$$

The results of the two previous sections can be expressed in a simplified way by exploiting the standard form of the CM. The CM of every tripartite system can be transformed in the following form via local unitary operators [25]

$$\mathcal{V} = \begin{bmatrix} r & 0 & d & 0 & f & f' \\ 0 & r & 0 & d' & f'' & f''' \\ d & 0 & b & 0 & e & e'' \\ 0 & d' & 0 & b & 0 & e' \\ f & f'' & e & 0 & c & 0 \\ f' & f''' & e' & e' & 0 & c \end{bmatrix}. \quad (35)$$

Applying this standard form to the CMs of the initial tripartite states in Eq. (20) is equivalent to set $\mathcal{R}_k = r_k \mathcal{I}$, $\mathcal{B}_k = b_k \mathcal{I}$, and $\mathcal{C}_k = c_k \mathcal{I}$ where \mathcal{I} is the 2×2 identity matrix. Also we have $\mathcal{D}_k = \text{diag}[d_k, d'_k]$, and

$$\mathcal{E}_k = \begin{bmatrix} e_k & e''_k \\ 0 & e'_k \end{bmatrix}, \quad \mathcal{F}_k = \begin{bmatrix} f_k & f'_k \\ f''_k & f'''_k \end{bmatrix},$$

where $k = 1, 2$. However, when all 2×2 submatrices of the CM \mathcal{V}_k are non-singular, the standard form of Eq. (35) gets an additional zero element $e''_k = 0$, i.e., we can write $\mathcal{E}_k = \text{diag}[e_k, e'_k]$ (cf. Ref. [26]).

As an entanglement monotone, we adopt the logarithmic negativity [21]

$$E_N = \max\{0, -\ln 2\eta^-\}, \quad (36)$$

where η^- is the minimum symplectic eigenvalue of the partially transposed CM. This is also known as minimum partially-transposed symplectic (PTS) eigenvalue and it is given by

$$\eta^- = \frac{1}{\sqrt{2}} \left(\Sigma(\mathcal{V}) - \sqrt{\Sigma(\mathcal{V})^2 - 4 \det \mathcal{V}} \right)^{\frac{1}{2}}, \quad (37)$$

where $\Sigma(\mathcal{V}) \equiv \det \mathcal{A} + \det \mathcal{B} - 2 \det \mathcal{C}$ can be extracted from the original CM expressed in the block form

$$\mathcal{V} = \begin{bmatrix} \mathcal{A} & \mathcal{C} \\ \mathcal{C}^\top & \mathcal{B} \end{bmatrix}. \quad (38)$$

It is clear that entanglement is present when $E_N > 0$ or equivalently $\eta^- < 1/2$. Furthermore, η^- is itself an entanglement monotone for Gaussian states, since it is monotonically related to E_N .

From the standard form of Eq. (35), we arrive at the following bipartite CMs for the two bipartite subsystems describing the two remote network nodes –Alice and Bob– and the certifying parties of Charlie,

$$\mathcal{V}_R = \frac{1}{b_1 + b_2} \begin{bmatrix} r_1(b_1 + b_2) - d_1^2 & 0 & d_1 d_2 & 0 \\ 0 & r_1(b_1 + b_2) - d_1'^2 & 0 & -d_1' d_2' \\ d_1 d_2 & 0 & r_2(b_1 + b_2) - d_2^2 & 0 \\ 0 & -d_1' d_2' & 0 & r_2(b_1 + b_2) - d_2'^2 \end{bmatrix}, \quad (39)$$

$$\mathcal{V}_C = \frac{1}{b_1 + b_2} \begin{bmatrix} c_1(b_1 + b_2) - e_1^2 & -e_1 e_1'' & e_1 e_2 & e_1 e_2'' \\ -e_1 e_1'' & c_1(b_1 + b_2) - (e_1'^2 + e_1''^2) & e_1' e_2 & e_1' e_2'' - e_1' e_2' \\ e_1 e_2 & e_1' e_2 & c_2(b_1 + b_2) - e_2^2 & -e_2 e_2'' \\ e_1 e_2'' & e_1' e_2'' - e_1' e_2' & -e_2 e_2'' & c_2(b_1 + b_2) - (e_2'^2 + e_2''^2) \end{bmatrix}. \quad (40)$$

From these matrices the remote-remote and certifying bipartite entanglement can be calculated, but their expression is too cumbersome to be reported here.

However, the explicit values for the entanglement monotone of the two bipartite states is significantly simplified when the initial tripartite states are identical, that is, when we start from a perfectly symmetric state between Alice and Bob. In this simpler case, we are able to derive compact formulas for the partial transpose symplectic eigenvalues. In fact one gets for the CM of the remote modes

$$\mathcal{V}_R = \begin{bmatrix} r - \frac{d^2}{2b} & & \frac{d^2}{2b} & \\ & r - \frac{d'^2}{2b} & & -\frac{d'^2}{2b} \\ \frac{d^2}{2b} & & r - \frac{d^2}{2b} & \\ & -\frac{d'^2}{2b} & & r - \frac{d'^2}{2b} \end{bmatrix}, \quad (41)$$

whose partial transpose CM $\mathcal{V}_R^{\text{PT}}$ has symplectic eigenvalues $\eta_R^- = b^{-1} \sqrt{\det \mathcal{V}_{RB}}$ and $\eta_R^+ = r$. On the other hand, the CM corresponding to the Charlie's test parties takes

the following form

$$\mathcal{V}_C = \begin{bmatrix} c - \frac{e^2}{2b} & -\frac{e e''}{2b} & \frac{e^2}{2b} & \frac{e e''}{2b} \\ -\frac{e e''}{2b} & c - \frac{e'^2 + e''^2}{2b} & \frac{e e'}{2b} & \frac{e' e'' - e'^2}{2b} \\ \frac{e^2}{2b} & \frac{e e'}{2b} & c - \frac{e^2}{2b} & -\frac{e e''}{2b} \\ \frac{e e''}{2b} & \frac{e' e'' - e'^2}{2b} & -\frac{e e''}{2b} & c - \frac{e'^2 + e''^2}{2b} \end{bmatrix}, \quad (42)$$

and the symplectic eigenvalues of the partial transpose CM $\mathcal{V}_C^{\text{PT}}$ are $\eta_C^\pm = (b\sqrt{2})^{-1} \left[\det \mathcal{V}_{BC} + b^2 c^2 \pm \sqrt{(b^2 c^2 - \det \mathcal{V}_{BC})^2 - (2bce'e'')^2} \right]^{\frac{1}{2}}$. In the above equations, \mathcal{V}_{RB} and \mathcal{V}_{BC} are the CM of the input subsystems given by

$$\mathcal{V}_{RB} = \begin{bmatrix} \mathcal{R} & \mathcal{D} \\ \mathcal{D}^\top & \mathcal{B} \end{bmatrix}, \quad \mathcal{V}_{BC} = \begin{bmatrix} \mathcal{B} & \mathcal{E} \\ \mathcal{E}^\top & \mathcal{C} \end{bmatrix}. \quad (43)$$

D. Tripartite certifying states

The condition for a successful, locally certified, entanglement swapping is obtained by finding the relation between the entanglement monotones η_R^- and η_C^- of the two bipartite subsystems, the remote modes at Alice and Bob sites, and the certifying modes in Charlie's hands. In the symmetric case, such a relation is given by their ratio,

$$\frac{\eta_C^-}{\eta_R^-} = \left[\frac{\det \mathcal{V}_{BC} + b^2 c^2 - \sqrt{(b^2 c^2 - \det \mathcal{V}_{BC})^2 - (2bce'e'')^2}}{2 \det \mathcal{V}_{RB}} \right]^{-\frac{1}{2}}. \quad (44)$$

If we consider the standard form of Ref. [26], i.e. $e_k'' = 0$, the relation between the remote sites entanglement and the certifying entanglement takes the following general form

$$\eta_R^- = \chi \eta_C^-, \quad (45)$$

where χ is a local symplectic invariant given by

$$\chi = \sqrt{\frac{\det \mathcal{V}_{RB}}{\det \mathcal{V}_{BC}}}. \quad (46)$$

This gives a sufficient condition for an indirectly measurable entanglement between Alice and Bob. In other words, if any entanglement between the certifying modes is detected by Charlie, the two distant and non-interacting modes are surely entangled, provided that the initial states are prepared so that $\chi < 1$. This sufficient condition can be expressed in terms of local purities of the system. The purity of a state is defined as $\mu(\varrho) = \text{Tr}(\varrho^2)$, where for an N -mode Gaussian state with CM $\mathcal{V}(\varrho)$ is

equal to

$$\mu(\varrho) = \frac{1}{2^N \sqrt{\det \mathcal{V}(\varrho)}}. \quad (47)$$

Therefore, it is easy to show that the minimum PTS eigenvalues of the bipartite remote sites and certifying modes are related to the local purities by the following equations

$$\eta_R^- = \frac{\mu_B}{2\mu_{RB}}, \quad \eta_C^- = \frac{\mu_B}{2\mu_{BC}}, \quad (48)$$

where μ_B is purity of the Bell mode, μ_{RB} that of the system formed by the mode in the remote site and that subject to the Bell measurement, and μ_{BC} that of the system formed by the two modes at Charlie's site. The sufficient and necessary condition for a successfully certified swapping process is to have for the output state $E_N^R > E_N^C > 0$. This condition can be rewritten from Eqs. (36) and (48) as

$$\mu_{RB} > \mu_{BC} > \mu_B. \quad (49)$$

Notice that this necessary and sufficient condition for ensuring that the swapping process is successfully executed and certified implies that the initial tripartite state should be prepared such that the certifying-Bell and remote-Bell bipartite subsystems are entangled. This can be verified as follows. According to Refs. [27, 28] the bipartite Gaussian state of the remote-Bell subsystem is inseparable if and only if

$$\mu_{RB} > \frac{\mu_R \mu_B}{\sqrt{\mu_R^2 + \mu_B^2 - \mu_R^2 \mu_B^2}}. \quad (50)$$

However, for every two variables x and y confined to $0 \leq x, y \leq 1$, the inequality

$$x \geq \frac{xy}{\sqrt{x^2 + y^2 - x^2 y^2}}$$

is always true. Therefore, by setting $x = \mu_B$ and $y = \mu_R$ and using Eq. (49), one has

$$\mu_{RB} > \mu_B \geq \frac{\mu_R \mu_B}{\sqrt{\mu_R^2 + \mu_B^2 - \mu_R^2 \mu_B^2}}, \quad (51)$$

which is just the necessary and sufficient condition for the entanglement of the remote-Bell subsystem. The same argument can be applied for the certifying-Bell subsystem by putting $x = \mu_B$ and $y = \mu_C$.

IV. THE OPTOMECHANICAL SYSTEM

We now apply this protocol to the case of an optomechanical system, in order to achieve entanglement between two distant macroscopic mechanical resonators. To this end, one prepares a tripartite optomechanical system involving a mechanical resonator coupled to two optical

modes both at Alice's and Bob's sites. The mechanical elements are the remote modes, while the optical modes are sent and shared with Charlie. Indeed, the goal of the protocol is the creation and certification of entanglement without any direct measurement on the mechanical elements, since quantum-limited measurement on mechanical modes maybe highly nontrivial [29, 30]. Therefore, it is necessary to exploit the two output optical modes as Bell and certifying modes (cf. Fig. 1(c)). This could be done by driving a single cavity mode, and then extracting two independent output optical modes by suitably filtering the outgoing field as in [31]. However, it is more efficient to drive *two different* cavity modes and filtering one output mode [32, 33] for each driven mode, and we shall consider this latter situation from now on. The two filtered optical modes are sent to Charlie for performing the Bell measurement and the certifying process. The latter is only a series of homodyne measurements, which will be carried out on the optical modes only.

A. The Hamiltonian

The optomechanical system is driven by two lasers which are appropriately detuned from the corresponding cavity mode. Thus, the Hamiltonian of the system is described by $\hat{H}_{\text{sys}} = \hat{H}_O + \hat{H}_M + \hat{H}_{OM} + \hat{H}_L$, where

$$\hat{H}_O = \hbar\omega_b \hat{a}_b^\dagger \hat{a}_b + \hbar\omega_c \hat{a}_c^\dagger \hat{a}_c \quad (52)$$

describes two different modes of the optical cavity with frequencies ω_b and ω_c and whose annihilation operators satisfy the usual bosonic commutation relations $[\hat{a}_k, \hat{a}_{k'}] = [\hat{a}_k^\dagger, \hat{a}_{k'}^\dagger] = 0$ and $[\hat{a}_k, \hat{a}_{k'}^\dagger] = \delta_{kk'}$ with $k, k' = b, c$. The mechanical element is described by

$$\hat{H}_M = \frac{\hbar\omega_M}{2} (\hat{p}^2 + \hat{q}^2), \quad (53)$$

which corresponds to a mechanical oscillator with mass m and resonance frequency ω_M . This means assuming that the cavity modes interact only with one resonant mode of the mechanical part of the system, which is justified when the detection bandwidth is chosen so that it includes only a single, isolated, mechanical resonance and mode-mode coupling is negligible [34]. In the above mechanical Hamiltonian, \hat{p} and \hat{q} are the dimensionless momentum and position of the micro-mechanical oscillator, respectively, such that $[\hat{q}, \hat{p}] = i$. The optomechanical interaction is described by

$$\hat{H}_{OM} = -\hbar\hat{q}(G_{0,b}\hat{a}_b^\dagger\hat{a}_b + G_{0,c}\hat{a}_c^\dagger\hat{a}_c), \quad (54)$$

where $G_{0,k}$ ($k = b, c$) are the single-photon optomechanical coupling constant. In the paradigmatic case of an optomechanical system formed by a Fabry-Perot cavity with a micromechanical mirror this coupling constants can be written in terms of the cavity length L as [33, 35]

$$G_{0,k} \equiv \frac{\omega_k}{L} \sqrt{\frac{\hbar}{m\omega_M}}. \quad (55)$$

Finally, the laser driving is described by

$$\hat{H}_L = i\hbar(E_b\hat{a}_b^\dagger e^{-i\omega_{L,b}} + E_c\hat{a}_c^\dagger e^{-i\omega_{L,c}}) + h.c., \quad (56)$$

where $|E_k| \equiv \sqrt{2\kappa_k P_{L,k}/\hbar\omega_{L,k}}$ is the driving rate of the cavity modes. Here $P_{L,k}$ is the laser input power and $\omega_{L,k}$ its frequency, while κ_k is the decay rate of the k th cavity mode.

B. Quantum Langevin equations

We use a quantum Langevin equation (QLE) approach to study the quantum dynamics of the optomechanical system at each site. The QLE can be derived from the full Hamiltonian of the system, i.e., by adding the Hamiltonian of the mechanical and optical reservoirs and their interaction with the system to \hat{H}_{sys} yielding, in a frame rotating at the frequencies of the two lasers [36],

$$\dot{\hat{q}} = \omega_M \hat{p} \quad (57a)$$

$$\dot{\hat{p}} = -\omega_M \hat{q} - \gamma_M \hat{p} + G_{0,b} \hat{a}_b^\dagger \hat{a}_b + G_{0,c} \hat{a}_c^\dagger \hat{a}_c + \hat{\xi} \quad (57b)$$

$$\dot{\hat{a}}_b = -[\kappa_b + i(\Delta_{0,b} - G_{0,b} \hat{q})] \hat{a}_b + E_b + \sqrt{2\kappa_b} \hat{a}_b^{\text{in}} \quad (57c)$$

$$\dot{\hat{a}}_c = -[\kappa_c + i(\Delta_{0,c} - G_{0,c} \hat{q})] \hat{a}_c + E_c + \sqrt{2\kappa_c} \hat{a}_c^{\text{in}} \quad (57d)$$

where $\Delta_{0,k} \equiv \omega_k - \omega_{L,k}$ is the detuning of the laser frequency with respect to the cavity modes. The mechanical noise operator $\hat{\xi}$ describes the zero-mean thermal noise, with correlation function

$$\langle \hat{\xi}(t) \hat{\xi}(t') \rangle = \frac{\gamma_M}{\omega_M} \int \frac{d\omega}{2\pi} \omega e^{-i\omega(t-t')} [1 + \coth(\frac{\hbar\omega}{2k_B T})], \quad (58)$$

where γ_M is the damping rate, k_B is the Boltzmann constant, and T is temperature of the mechanical reservoir. The only non-vanishing correlation function of the noise operators acting on the optical modes due to the vacuum fluctuations are

$$\langle \hat{a}_k(t) \hat{a}_{k'}^\dagger(t) \rangle = \delta_{kk'} \delta(t-t'). \quad (59)$$

In the present proposal, non-local entanglement between the two non-interacting mechanical resonators at Alice and Bob site is created by swapping an initially present optomechanical entanglement between the mechanical mode and the Bell output optical mode. This latter entanglement is known to be strong and robust in the case of strong optomechanical coupling [11, 37, 38], and a straightforward way to enter this regime [39, 40] is to intensely drive the optical modes and to consider the linearized quantum fluctuations around the resulting classical steady state. By assuming high intensity intracavity fields one approximates the cavity mode operators as a steady state coherent field with large amplitude and quantum fluctuations around it. Therefore, for every operator \hat{o} one can write $\hat{o} = o_s + \delta\hat{o}$ and get the following

classical steady state values

$$p_s = 0, \quad (60a)$$

$$q_s = \frac{1}{\omega_M} (G_{0,b} |a_{s,b}|^2 + G_{0,c} |a_{s,c}|^2), \quad (60b)$$

$$a_{s,k} = \frac{E_k}{\kappa_k + i\Delta_k}, \quad (k = b, c), \quad (60c)$$

where the effective detuning are defined as $\Delta_k \equiv \Delta_{0,k} - G_{0,k} q_s$.

The linearized dynamics of the small quantum fluctuations of the optomechanical system can be described in compact form in terms of the vector of fluctuations $\hat{\mathbf{u}} \equiv [\delta\hat{q}, \delta\hat{p}, \delta\hat{x}_b, \delta\hat{y}_b, \delta\hat{x}_c, \delta\hat{y}_c]^\top$ as

$$\dot{\hat{\mathbf{u}}} = \mathcal{K} \hat{\mathbf{u}} + \hat{\mathbf{n}}, \quad (61)$$

where $\hat{\mathbf{n}} \equiv [0, \hat{\xi}, \sqrt{2\kappa_b} \hat{x}_b^{\text{in}}, \sqrt{2\kappa_b} \hat{y}_b^{\text{in}}, \sqrt{2\kappa_c} \hat{x}_c^{\text{in}}, \sqrt{2\kappa_c} \hat{y}_c^{\text{in}}]^\top$ is the noise vector, and \mathcal{K} is the matrix of coefficients, given by

$$\mathcal{K} \equiv \begin{bmatrix} 0 & \omega_M & 0 & 0 & 0 & 0 \\ -\omega_M & -\gamma_M & G_b & 0 & G_c & 0 \\ 0 & 0 & -\kappa_b & \Delta_b & 0 & 0 \\ G_b & 0 & -\Delta_b & -\kappa_b & 0 & 0 \\ 0 & 0 & 0 & 0 & -\kappa_c & \Delta_c \\ G_c & 0 & 0 & 0 & -\Delta_c & -\kappa_c \end{bmatrix}, \quad (62)$$

where $G_k \equiv \sqrt{2} G_{0,k} a_{s,k}$ are the effective optomechanical couplings which can be made large and tunable by varying the stationary intracavity amplitudes $a_{s,k}$.

The steady state of the tripartite optomechanical system exists and it is stable if all the eigenvalues of the drift matrix \mathcal{K} have negative real parts. The parameter region under which stability occurs can be obtained from the Routh–Hurwitz criterion [41], but the inequalities that come out are quite involved. However, the present bichromatically driven system has a regime in which the system is always stable, achieved when $G_b = G_c$ and $\Delta_b = -\Delta_c$, where there is a balance between a stabilizing “cooling” cavity mode with positive detuning and a “heating” cavity mode with negative detuning. Ref. [33] has shown that this bichromatically driven system in this regime provides a robust and significative optomechanical entanglement and we assume to operate in such a regime for a possible implementation of the proposed entanglement swapping protocol.

C. Optomechanical entanglement of output modes

Charlie performs his Bell and certifying measurements on the optical modes at the output of the optomechanical cavities, which can always be optimized with filters which, if appropriately chosen, may lead to a significative increase of the entanglement with respect to their intracavity counterpart [31]. The effective, filtered output modes are defined by the following bosonic annihilation

operators

$$\hat{a}_k^{\text{out}}(t) = \int_{t_0}^t h_k(t-s) [\sqrt{2\kappa_k} \delta \hat{a}_k(t) - \hat{a}_k^{\text{in}}(t)] ds \quad (63)$$

where $h_k(t)$ is a causal filter function defining the output modes [31]. In fact, \hat{a}_k^{out} is a standard photon annihilation operator, implying the normalization condition $\int |h_k(t)|^2 dt = 1$. A simple choice is

$$h_k(t) = \sqrt{\frac{2}{\tau_k}} \Theta(t) \exp \left[-\left(\frac{1}{\tau_k} + i\Omega_k \right) t \right], \quad (64)$$

where $\Theta(t)$ is the Heaviside step function, $1/\tau_k$ is the bandwidth of the filter, and Ω_k is the central frequency (measured with respect to the frequency of the corresponding driving field).

The stationary entanglement in the tripartite Gaussian state of the selected output optical modes and the mechanical resonator is determined by its 6×6 CM

$$\mathcal{V}_{ij}^{\text{out}} = \frac{1}{2} \langle \hat{u}_i^{\text{out}}(\infty) \hat{u}_j^{\text{out}}(\infty) + \hat{u}_j^{\text{out}}(\infty) \hat{u}_i^{\text{out}}(\infty) \rangle, \quad (65)$$

where $\hat{\mathbf{u}}^{\text{out}} \equiv [\delta \hat{q}, \delta \hat{p}, \hat{x}_b^{\text{out}}, \hat{y}_b^{\text{out}}, \hat{x}_c^{\text{out}}, \hat{y}_c^{\text{out}}]^T$ is the vector formed by the output field quadratures and by the mechanical operators. This output CM can be expressed in terms of a frequency integral as [31, 33]

$$\mathcal{V}^{\text{out}} = \int d\omega \tilde{\mathcal{T}}(\omega) [\tilde{\mathcal{N}}(\omega) + \mathcal{P}_{\text{out}}] \mathcal{Q}(\omega) \times [\tilde{\mathcal{N}}(\omega)^\dagger + \mathcal{P}_{\text{out}}] \tilde{\mathcal{T}}(\omega)^\dagger, \quad (66)$$

where $\tilde{\mathcal{N}}(\omega) \equiv (i\omega \mathcal{I} + \mathcal{K})^{-1}$ and $\tilde{\mathcal{T}}(\omega)$ is the Fourier transform of

$$\mathcal{T}(t) = \begin{bmatrix} \delta(t) & 0 & 0 & 0 & 0 & 0 \\ 0 & \delta(t) & 0 & 0 & 0 & 0 \\ 0 & 0 & \sqrt{2\kappa_b} h_b^{\Re}(t) & -\sqrt{2\kappa_b} h_b^{\Im}(t) & 0 & 0 \\ 0 & 0 & \sqrt{2\kappa_b} h_b^{\Im}(t) & \sqrt{2\kappa_b} h_b^{\Re}(t) & 0 & 0 \\ 0 & 0 & 0 & 0 & \sqrt{2\kappa_c} h_c^{\Re}(t) & -\sqrt{2\kappa_c} h_c^{\Im}(t) \\ 0 & 0 & 0 & 0 & \sqrt{2\kappa_c} h_c^{\Im}(t) & \sqrt{2\kappa_c} h_c^{\Re}(t) \end{bmatrix}. \quad (67)$$

$\mathcal{P} \equiv \text{diag}[0, 0, 1/2\kappa_b, 1/2\kappa_b, 1/2\kappa_c, 1/2\kappa_c]$ is the projector onto the optical quadratures, while $\mathcal{Q}(\omega)$ is the diffusion matrix of the system, given by

$$\mathcal{Q}(\omega) = \text{diag} \left[0, \frac{\gamma_M}{\omega_M} \omega \coth \left(\frac{\hbar \omega}{2k_B T} \right), \kappa_b, \kappa_b, \kappa_c, \kappa_c \right]. \quad (68)$$

Using the CM one can analyze the bipartite entanglement within the three different bipartitions of the system when one of the three modes is traced out, and also the tripartite entanglement.

D. Entanglement of the micromechanical resonators by entanglement swapping

An initially present optomechanical entanglement between the mechanical resonator and an output cavity mode (in each tripartite system) can be swapped into an entanglement between the two remote mechanical oscillators by means of the Bell measurement on the two optical modes. Furthermore, such an entanglement can be locally verified and certified by Charlie when there is a nonzero entanglement between the two optical certifying output fields, one from Alice and the other from Bob. From the discussion of Sec. III, the two above conditions are achieved when the tripartite optomechanical systems at each site is initially in a state satisfying the certifying condition of Eq. (46), involving only purities. Therefore,

we have to determine an experimentally achievable parameter set in which such conditions are satisfied so that the proposed generalized swapping protocol can be successfully implemented.

Still restricting to the symmetric case of initially identical states at Alice and Bob sites, one has the following classification of tripartite optomechanical states:

- Class 1) certifiable* : $\mu_{\text{RB}} > \mu_{\text{BC}} > \mu_{\text{B}}$
- Class 2) not certifiable* : $\mu_{\text{RB}} > \mu_{\text{B}} \ \& \ \mu_{\text{BC}} < \mu_{\text{B}}$
- Class 3) wrong swapping* : $\begin{cases} \mu_{\text{BC}} > \mu_{\text{RB}} > \mu_{\text{B}} \\ \mu_{\text{BC}} > \mu_{\text{B}} \ \& \ \mu_{\text{RB}} < \mu_{\text{B}} \end{cases}$
- Class 4) no swapping* : $\mu_{\text{RB}} < \mu_{\text{B}} \ \& \ \mu_{\text{BC}} < \mu_{\text{B}}$

The first case is the desired class of tripartite *certifying* states [22] which guarantees a successful implementation of the protocol. In the second case, the two remote mechanical resonators are entangled after the protocol, but there is no entanglement between the certifying optical modes. Therefore, the success of entanglement swapping cannot be locally certified. In the third case, which we call “wrong swapping” the Bell and certifying modes are more entangled than the remote and Bell modes; in this case one has an entangled pair of certifying modes, but this entanglement is greater than the value of the mechanical–mechanical entanglement which can be either zero or nonzero, and therefore one cannot say anything certain about the entanglement between the remote modes. In this case in fact, instead of having

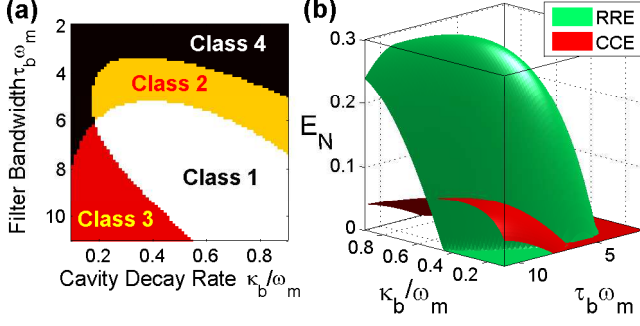


FIG. 2. (Color online) (a) Classification of the input tripartite states, and (b) value of the E_N for the entanglement between the remote modes ‘RRE’ and the certifying modes ‘CCE’ as a function of the cavity decay rates and filtering bandwidths. The system parameters are: input powers $P_b = 4$ mW and $P_c = 4.5$ mW, detuning of the lasers $\Delta_b = -\Delta_c = -\omega_M$, filtering inverse bandwidths are chosen so that $\tau_c = \tau_b/6$, and the decay rate are chosen to be equal $\kappa_c = \kappa_b$. See the text for the other parameters.

most entangled mechanical resonators, one gets two optical modes with higher entanglement. The fourth case is the worst situation when no swapping occurs because we do not have the necessary optomechanical entanglement to start with.

The desired certifying condition of Eq. (46) is satisfied if we appropriately choose the detuning and filter the output modes. In fact, we have found that the mechanical–mechanical entanglement is larger when we drive the cavity Bell mode with a blue-detuned laser ($\Delta_b < 0$) and the certifying mode by a red-detuned laser ($\Delta_c > 0$). Indeed, it is shown in Ref. [33] that in this case the remote–Bell optomechanical entanglement is larger and both required conditions of large mechanical–mechanical entanglement and smaller certifying entanglement are easier to achieve. Let us verify this by considering an optomechanical system with state-of-the-art parameter values. The system is composed of a Fabry–Pérot cavity with $L = 1$ mm length, whose movable mirror has an effective mass $m = 10$ ng, resonance frequency of $\omega_M/2\pi = 10$ MHz, quality factor $Q_M = \gamma_M/\omega_M = 10^5$, and coupled to a reservoir at temperature $T = 0.4$ K. We consider two lasers driving two adjacent cavity modes with wavelengths $\lambda_b = 810.045$ nm and $\lambda_c = 810.373$ nm and with the above-mentioned choice of opposite detunings, $\Delta_b = -\Delta_c = -\omega_M$. Moreover the output optical modes corresponding to the Bell modes are filtered in order to be centered around the Stokes sideband, while the certifying modes are centered around the anti-Stokes sideband, i.e., we have $\Omega_b = -\Omega_c = -\omega_M$. We now study the properties of the initial tripartite Gaussian state with the above parameter choice, as a function of the remaining parameters, that is, the cavity bandwidths κ_k , the input powers P_k , and the bandwidth of the filtered output modes, $1/\tau_k$, $k = b, c$.

Fig. 2(a) shows the class of the initial Gaussian tri-

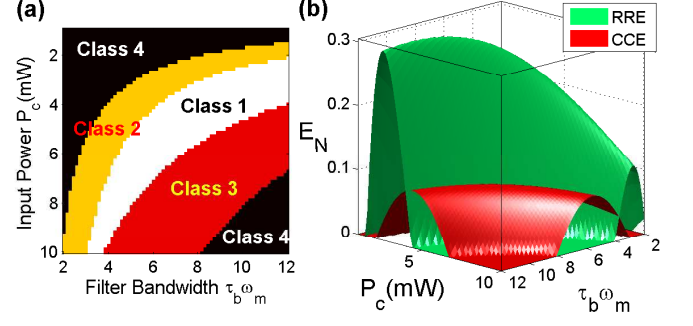


FIG. 3. (Color online) (a) Classification of the input tripartite states, and (b) value of the E_N for the entanglement between the remote modes ‘RRE’ and the certifying modes ‘CCE’ as a function of laser power and filtering bandwidths. The cavity decay rates are fixed, $\kappa_b = \kappa_c = 0.5\omega_M$, detuning of the lasers are $\Delta_b = -\Delta_c = -\omega_M$. The filtering inverse bandwidth are chosen so that $\tau_c = \tau_b/5$, while the laser powers are chosen so that $P_c - P_b = 0.5$ mW. See the text for the other parameters.

partite state at fixed input powers $P_b = 4$ mW, $P_c = 4.5$ mW, in a chosen interval of cavity bandwidths (here assumed to be equal $\kappa_b = \kappa_c$) and of inverse output bandwidths (here chosen so that $\tau_c = \tau_b/6$). The white region corresponds to the desired class 1 of certifying states, leading to a successful entanglement swapping certifiable with local measurements. Fig. 2(b) refers to the same parameter region and describes the “output” of the protocol. In fact, it shows the logarithmic negativity E_N of the mechanical–mechanical entanglement (the green surface named as ‘RRE’), and of the certifying optical modes (the red surface named as ‘CCE’). This latter figure shows that a log-negativity RRE of $E_N \simeq 0.3$ for the remote modes can be certified by $E_N \simeq 0.05$ for the certifying modes.

Then, Fig. 3 shows the class of the initial Gaussian tripartite state and the protocol output as a function of the input powers and filtering bandwidths (now assuming $\tau_c = \tau_b/5$), at fixed and identical cavity bandwidths $\kappa_b = \kappa_c = 0.5\omega_M$. In this case, the desired certifying state region of class 1 is the white strip shown in Fig. 3(a), while Fig. 3(b) shows again E_N of the mechanical–mechanical entanglement (green surface ‘RRE’), and of the certifying optical modes (red surface ‘CCE’). Fig. 3(b) indicates that a remote entanglement of $E_N \simeq 0.2$ can be certified by an entanglement between the two certifying optical modes $E_N \simeq 0.1$.

V. CONCLUSION

We have described in detail an extension of the entanglement swapping protocol which can be applied to an appropriate class of tripartite states. This protocol allows to swap an initially available entanglement to two sites which have never interacted and to *certify* it by measuring locally the entanglement between two ancil-

lary modes at the same site where the Bell measurement is carried out. We determine and characterize the class of certifying states in the case of tripartite Gaussian CV states, showing that they can be fully identified in terms of local and bipartite purities [22].

We have then discussed the application of the proposed swapping protocol with local certification to identical tripartite Gaussian states of two optomechanical systems. The protocol is applied to generate entanglement between two mechanical resonators at two remote sites, using two output optical cavity modes from each site for carrying out both the Bell measurement, for swapping the entanglement, and the homodyne measurements for

certifying the success of the protocol. In this work we considered detections performed on optical modes but our analysis could be extended to other types of systems, for instance to the microwave modes of a modified coplanar waveguide [42].

ACKNOWLEDGMENTS

This work has been supported by the European Commission (ITN-Marie Curie project cQOM, FET-Open Project iQUOEMS), MIUR (PRIN 2010-2011), EPSRC (through HIPERCOM, EP/J00796X/1 and qDATA, EP/L011298/1) and The Leverhulme Trust.

-
- [1] R. Horodecki, P. Horodecki, M. Horodecki, and K. Horodecki, *Rev. Mod. Phys.*, **81**, 865 (2009).
 - [2] C. Weedbrook, S. Pirandola, R. Garcia-Patron, N. J. Cerf, T. C. Ralph, J. H. Shapiro, and S. Lloyd, *Rev. Mod. Phys.*, **84**, 621 (2012).
 - [3] S. L. Braunstein and P. van Loock, *Rev. Mod. Phys.*, **77**, 513 (2005).
 - [4] M. A. Nielsen and I. L. Chuang, *Quantum Computation and Quantum Information* (Cambridge University Press, 2000).
 - [5] Q. A. Turchette, C. S. Wood, B. E. King, C. J. Myatt, D. Leibfried, W. M. Itano, C. Monroe, and D. J. Wineland, *Phys. Rev. Lett.*, **81**, 3631 (1998).
 - [6] D. Jaksch, H.-J. Briegel, J. I. Cirac, C. W. Gardiner, and P. Zoller, *Phys. Rev. Lett.*, **82**, 1975 (1999).
 - [7] S.-B. Zheng and G.-C. Guo, *Phys. Rev. Lett.*, **85**, 2392 (2000).
 - [8] K. C. Lee, M. R. Sprague, B. J. Sussman, J. Nunn, N. K. Langford, X.-M. Jin, T. Champion, P. Michelberger, K. F. Reim, D. England, D. Jaksch, and I. A. Walmsley, *Science*, **334**, 1253 (2011).
 - [9] J. Yin, J.-G. Ren, H. Lu, Y. Cao, H.-L. Yong, Y.-P. Wu, C. Liu, S.-K. Liao, F. Zhou, Y. Jiang, X.-D. Cai, P. Xu, G.-S. Pan, J.-J. Jia, Y.-M. Huang, H. Yin, J.-Y. Wang, Y.-A. Chen, and C.-Z. P. J.-W. Pan, *Nature*, **488**, 185 (2012).
 - [10] X. Ma, T. Herbst, T. Scheidl, D. Wang, S. Kropatschek, W. Naylor, A. Mech, B. Wittmann, J. Kofler, E. Anisimova, V. Makarov, T. Jennewein, R. Ursin, and A. Zeilinger, *Nature (London)*, **489**, 269 (2012).
 - [11] D. Vitali, S. Gigan, A. Ferreira, H. R. Bohm, P. Tombesi, A. Guerreiro, V. Vedral, A. Zeilinger, and M. Aspelmeyer, *Phys. Rev. Lett.*, **98**, 030405 (2007).
 - [12] J. I. Cirac, P. Zoller, H. J. Kimble, and H. Mabuchi, *Phys. Rev. Lett.*, **78**, 3221 (1997).
 - [13] J.-W. Pan, D. Bouwmeester, H. Weinfurter, and A. Zeilinger, *Phys. Rev. Lett.*, **80**, 3891 (1998).
 - [14] X. Jia, X. Su, Q. Pan, J. Gao, C. Xie, and K. Peng, *Phys. Rev. Lett.*, **93**, 250503 (2004).
 - [15] N. Takei, H. Yonezawa, T. Aoki, and A. Furusawa, *Phys. Rev. Lett.*, **94**, 220502 (2005).
 - [16] S. Pirandola and S. Mancini, *Laser Physics*, **16**, 1418 (2006).
 - [17] B. Julsgaard, A. Kozhekin, and E. S. Polzik, *Nature*, **413**, 400 (2001).
 - [18] O. Romero-Isart, A. C. Pflanzner, F. Blaser, R. Kaltenbaek, N. Kiesel, M. Aspelmeyer, and J. I. Cirac, *Phys. Rev. Lett.*, **107**, 020405 (2011).
 - [19] O. Romero-Isart, A. C. Pflanzner, M. L. Juan, R. Quidant, N. Kiesel, M. Aspelmeyer, and J. I. Cirac, *Phys. Rev. A*, **83**, 013803 (2011).
 - [20] S. Pirandola, D. Vitali, P. Tombesi, and S. Lloyd, *Phys. Rev. Lett.*, **97**, 150403 (2006).
 - [21] G. Vidal and R. F. Werner, *Phys. Rev. A*, **65**, 032314 (2002).
 - [22] M. Abdi, S. Pirandola, P. Tombesi, and D. Vitali, *Phys. Rev. Lett.*, **109**, 143601 (2012).
 - [23] P. van Loock and S. L. Braunstein, *Phys. Rev. A*, **61**, 010302(R) (1999).
 - [24] J. Hoelscher-Obermaier and P. van Loock, *Phys. Rev. A*, **83**, 012319 (2011).
 - [25] G. Adesso, A. Serafini, and F. Illuminati, *Phys. Rev. A*, **73**, 032345 (2006).
 - [26] L. Wang, S.-S. Li, and H.-Z. Zheng, *Phys. Rev. A*, **67**, 062317 (2003).
 - [27] G. Adesso, A. Serafini, and F. Illuminati, *Phys. Rev. A*, **70**, 022318 (2004).
 - [28] G. Adesso, A. Serafini, and F. Illuminati, *Phys. Rev. Lett.*, **92**, 087901 (2004).
 - [29] M. Paternostro, G. De Chiara, and G. M. Palma, *Phys. Rev. Lett.*, **104**, 243602 (2010).
 - [30] G. De Chiara, M. Paternostro, and G. M. Palma, *Phys. Rev. A*, **83**, 052324 (2011).
 - [31] C. Genes, A. Mari, P. Tombesi, and D. Vitali, *Phys. Rev. A*, **78**, 032316 (2008).
 - [32] V. Giovannetti, S. Mancini, and P. Tombesi, *Europhys. Lett.*, **54**, 559 (2001).
 - [33] C. Genes, A. Mari, D. Vitali, and P. Tombesi, *Adv. At. Mol. Opt. Phys.*, **57**, 33 (2009).
 - [34] C. Genes, D. Vitali, and P. Tombesi, *New J. Phys.*, **10**, 095009 (2008).
 - [35] M. Aspelmeyer, P. Meystre, and K. Schwab, *Phys. Today*, **65** (7), 29 (2012).
 - [36] V. Giovannetti and D. Vitali, *Phys. Rev. A*, **63**, 023812 (2001).
 - [37] S. Hofer, W. Wieczorek, M. Aspelmeyer, and K. Hammerer, *Phys. Rev. A*, **84**, 052327 (2011).

- [38] M. Abdi, S. Barzanjeh, P. Tombesi, and D. Vitali, Phys. Rev. A, **84**, 032325 (2011).
- [39] S. Gröblacher, K. Hammerer, M. R. Vanner, and M. Aspelmeyer, Nature (London), **460**, 724 (2009).
- [40] J. D. Teufel, D. Li, M. S. Allman, K. Cicak, A. J. Sirois, J. D. Whittaker, and R. W. Simmonds, Nature (London), **471**, 204 (2011).
- [41] K. Ogata, *Modern Control Engineering* (Prentice Hall, 2010).
- [42] S. Barzanjeh, M. Abdi, G. J. Milburn, P. Tombesi, and D. Vitali, Phys. Rev. Lett., **109**, 130503 (2012).